Video Article

Cryogenic Liquid Jets for High Repetition Rate Discovery Science

Chandra B. Curry*[1,2], Christopher Schoenwaelder*[1,3], Sebastian Goede[4], Jongjin B. Kim[1], Martin Rehwald[5,6], Franziska Treffert[1,7], Karl Zeil[5], Siegfried H. Glenzer[1], Maxence Gauthier[1]

[1]SLAC National Accelerator Laboratory

[2]University of Alberta

[3]Friedrich-Alexander-Universität Erlangen-Nürnberg

[4]European XFEL

[5]Helmholtz-Zentrum Dresden-Rossendorf

[6]Technische Universität Dresden

[7]Technische Universität Darmstadt

*These authors contributed equally

Correspondence to: Siegfried H. Glenzer at glenzer@slac.stanford.edu

URL: https://www.jove.com/video/61130
DOI: doi:10.3791/61130

Keywords: Engineering, Issue 159, cryogenic liquids, fluid dynamics, liquid jets, laser-driven ion acceleration, high repetition rate

Date Published: 5/9/2020

Citation: Curry, C.B., Schoenwaelder, C., Goede, S., Kim, J.B., Rehwald, M., Treffert, F., Zeil, K., Glenzer, S.H., Gauthier, M. Cryogenic Liquid Jets for High Repetition Rate Discovery Science. *J. Vis. Exp.* (159), e61130, doi:10.3791/61130 (2020).

Abstract

This protocol presents a detailed procedure for the operation of continuous, micron-sized cryogenic cylindrical and planar liquid jets. When operated as described here, the jet exhibits high laminarity and stability for centimeters. Successful operation of a cryogenic liquid jet in the Rayleigh regime requires a basic understanding of fluid dynamics and thermodynamics at cryogenic temperatures. Theoretical calculations and typical empirical values are provided as a guide to design a comparable system. This report identifies the importance of both cleanliness during cryogenic source assembly and stability of the cryogenic source temperature once liquefied. The system can be used for high repetition rate laser-driven proton acceleration, with an envisioned application in proton therapy. Other applications include laboratory astrophysics, materials science, and next-generation particle accelerators.

Introduction

The goal of this method is to produce a high-speed, cryogenic liquid flow consisting of pure elements or chemical compounds. Since cryogenic liquids evaporate at ambient temperature and pressure, residual samples from operation at high repetition rates (e.g., 1 kHz) can be entirely evacuated from the vacuum chamber[1]. Based on the initial work by Grisenti et al.[2], this system was first developed using cryogenic hydrogen for high intensity laser-driven proton acceleration[3]. It has subsequently been extended to other gases and used in a number of experiments, including: ion acceleration[4,5], answering questions in plasma physics such as plasma instabilities[6], rapid crystallization and phase transitions in hydrogen[7] and deuterium, and meV inelastic X-ray scattering[8] to resolve acoustic waves in argon in the Matter in Extreme Conditions (MEC) instrument at the Linac Coherent Light Source (LCLS)[9].

Until now, other alternative methods have been developed to generate high repetition rate solid cryogenic hydrogen and deuterium samples. Garcia et al. developed a method in which hydrogen is liquefied and solidified in a reservoir and extruded through an aperture[10]. Due to the high pressure required for extrusion, the minimum sample thickness demonstrated (to date) is 62 µm[11]. This system also exhibits large spatial jitter[12]. More recently, Polz et al. produced a cryogenic hydrogen jet through a glass capillary nozzle using a sample gas backing pressure of 435 psig (pounds per square inch, gauge). The resulting 10 µm cylindrical jet is continuous but appears highly rippled[13].

Presented here is a method that produces cylindrical (diameter = 5-10 µm) and planar jets with various aspect ratios (1-7 µm x 10-40 µm). The pointing jitter increases linearly as a function of distance from the aperture[5]. Fluid properties and the equation of state dictate the elements and chemical compounds that can be operated in this system. For example, methane cannot form a continuous jet due to Rayleigh breakup, but it can be used as droplets[14]. Moreover, the optimal pressure and temperature conditions vary significantly among aperture dimensions. The following paragraphs provide the theory needed to produce laminar, turbulent-free cryogenic hydrogen jets. This can be extended to other gases.

The cryogenic jet system consists of three main subsystems: (1) sample gas delivery, (2) vacuum, and (3) cryostat and cryogenic source. The system depicted in **Figure 1** has been designed to be highly adaptable for installation in different vacuum chambers.

The gas delivery system is comprised of an ultra-high purity compressed gas cylinder, gas regulator, and mass flow controller. The backing pressure of the sample gas is set by the gas regulator, while the mass flow controller is used to measure and restrict the gas flow delivered to the system. The sample gas is first filtered in a liquid nitrogen cold trap to freeze out contaminant gases and water vapor. A second in-line particulate filter prevents debris from entering the final segment of the gas line.

Turbomolecular pumps backed with high pumping speed scroll pumps maintain high vacuum conditions in the sample chamber. The chamber and foreline vacuum pressures are monitored using vacuum gauges V1 and V2, respectively. It should be noted that operating the cryogenic jet introduces a substantial gas load (proportional to the total sample flow) into the vacuum system when the liquid vaporizes.

A proven method to reduce the gas load is to capture the residual liquid before bulk vaporization can occur. The jet catcher system consists of an independent vacuum line terminated by an ø800 µm differential pumping aperture located up to 20 mm from the cryogenic source cap. The line is evacuated with a pump that exhibits optimal efficiency in the 1 x 10^{-2} mBar range (i.e., a roots blower vacuum pump or hybrid turbomolecular pump) and is monitored by a vacuum gauge V3. More recently, the catcher has allowed cryogenic hydrogen jets of up to 7 µm x 13 µm to be operated with two orders of magnitude improvement to the vacuum chamber pressure.

A fixed length, continuous flow liquid helium cryostat is used to cool the source to cryogenic temperatures. Liquid helium is drawn from a supply dewar using a transfer line. The return flow is connected to an adjustable flowmeter panel to regulate the cooling power. The temperature of the cold finger and cryogenic source is measured with four lead silicon diode temperature sensors. A proportional-integral-derivative (P-I-D) temperature controller delivers variable voltage to a heater installed near the cold finger to adjust and stabilize the temperature. The sample gas enters the vacuum chamber through a custom feedthrough on the cryostat flange. Inside the chamber, the gas line wraps around the cryostat to precool the gas before connecting to a fixed gas line on the cryogenic source assembly. Stainless steel screws and a 51 µm thick layer of indium thermally seal the cryogenic source to the cold finger.

The cryogenic source (**Figure 2**) consists of six main components: a (1) sample gas line, (2) source body, (3) source flange with in-line particulate filter, (4) aperture, (5) ferrule, and (6) cap. The source body contains a void, which acts as the sample reservoir. A threaded Swagelok sintered 0.5 µm stainless steel filter prevents any debris or solidified contaminants from entering the liquid channel and obstructing the aperture. A thicker, 76 µm thick indium ring is placed between the aperture and liquid channel to increase the deformation length and reliably seal the aperture. When the cap is threaded onto the source flange, the indium is compressed to form a liquid and thermal seal. The ferrule and source cap center the aperture during installation.

There are a number of overall considerations in the initial design of a system for cryogenic liquid jets operated in the continuous, laminar regime. Users must estimate the total cooling power of the cryostat, thermal properties of the cryogenic source design, vacuum system performance, and liquid temperature and pressure. Provided below is the theoretical framework required.

Cooling power considerations

1) Liquefying hydrogen[15]: the minimum cooling power required to liquify hydrogen from 300 K to a temperature T_c can be roughly estimated using the following equation:

$$P_{liq} = L_h(T_l(p)) + \int_{T_c}^{300K} C_p(T)dT$$

Where: C_p is the specific heat at constant pressure p, and L_h the latent heat of vaporization of H_2 at the pressure-dependent liquefaction temperature T_l. For instance, a cryogenic hydrogen jet operated at 60 psig gas pressure and cooled down to 17 K requires a minimum of 4013 kJ/kg. With a hydrogen gas flow of 150 sccm (standard cubic centimeters per second), this corresponds to a heat of $\sim$ 0.9 W.

It should be noted that the liquefaction process contributes only one-tenth of the total cooling power required. To reduce the heat load on the cryostat, the gas can be precooled to an intermediate temperature before entering the source body.

2) Radiative heat: to maintain the cryogenic source at a temperature T_c, the cryostat needs to compensate for radiative heating. This can be estimated by balancing the difference of emitted and absorbed blackbody radiation using the following equation:

$$P_{rad} = A\sigma(T_{vc}^4 - T_c^4)$$

Where: *A* is the area of the source body, σ is the Stefan-Boltzmann constant, and T_{vc} is the temperature of the vacuum chamber. For example, a typical jet source of *A* = 50 cm^2 cooled down to 17 K requires a minimum cooling power of 2.3 W. T_{vc} can be locally decreased by adding an actively cooled radiation shield covering a substantial part of the cryogenic source.

3) Residual gas conduction: although thermal radiation is dominant in ultra-high vacuum conditions, the contribution due to conduction in the residual gas becomes non-negligible during jet operation. The liquid jet introduces substantial gas load in the chamber, resulting in an increase in vacuum pressure. The net heat loss from thermal conduction of the gas at a pressure *p* is calculated using the following equation:

$$P_{gas} = A\alpha\Omega\, p(\mathrm{T_{vc}} - \mathrm{T_c})$$

Where: Ω is a coefficient depending on the gas species (~3.85 x 10^{-2} W/cm^2/K/mBar for H_2), and α is the accommodation coefficient that depends on the gas species, geometry of the source, and temperature of the source and the gas[16,17]. When operating a cryogenic hydrogen jet at 17 K, assuming a cylindrical geometry of the source and that hydrogen is the main gas present in the vacuum chamber, gas conduction generates heat that can be estimated using the following equation:

$$P_{gas}/A \approx 10.9 * p_{mBar}\ W/cm^2$$

For example, gas conduction at a vacuum pressure of 4.2 x 10^{-3} mBar generates as much heat as thermal radiation. Therefore, the vacuum pressure is generally kept below 1 x 10^{-3} mBar during jet operation, adding a ~0.55 W heat load to the system (*A* = 50 cm^2).

The gas load introduced in the chamber during operation is obtained by the flow of the cryogenic jet. The resulting vacuum pressure is then determined by the effective pumping speed of the vacuum system and volume of the vacuum chamber.

To operate the cryogenic jet, the cryostat has to generate sufficient cooling power to compensate for the different heat sources above (e.g., 3.75 W), not including the heat losses of the cryostat system itself. Note that the cryostat efficiency also strongly depends on the desired cold finger temperature.

Estimating jet parameters

To establish continuous laminar flow, several conditions must be satisfied. For brevity, the case of a cylindrical liquid flow is shown here. The formation of planar jets involves additional forces, resulting in a more complex derivation that is beyond the scope of this paper[18].

1) Pressure-speed relationship: for incompressible liquid flows, conservation of energy yields the Bernoulli equation, as follows:

$$\frac{1}{2}\rho v^2 + \rho g z + p = const.$$

Where: ρ is the fluid atomic density, v is the fluid velocity, gz is gravitational potential energy, and p is the pressure. Applying the Bernoulli equation across the aperture, the functional relationship between the jet velocity and sample backing pressure can be estimated using the following equation:

$$v \simeq \sqrt{2p/\rho}$$

2) Jet operation regime: the regime of a cylindrical liquid jet can be inferred using the Reynolds and the Ohnesorge numbers. The Reynolds number, defined as the ratio between the inertial and viscous forces within the fluid, is calculated using the following equation:

$$R_e = \frac{\rho v d_0}{\eta}$$

Where: ρ, v, d_0, and η are the density, speed, diameter, and dynamic viscosity of the fluid, respectively. Laminar flow occurs when the Reynolds number is less than ~2,000. Similarly, the Weber number compares the relative magnitude of the inertia to the surface tension and is calculated using the following equation:

$$W_e = \frac{\rho v^2 d_0}{\sigma}$$

Where: σ is the surface tension of the liquid. The Ohnesorge number is then calculated as follows:

$$\mathrm{Oh} = \frac{\sqrt{W_e}}{R_e}$$

This velocity-independent quantity is used in combination with the Reynolds number to identify the four liquid jet regimes: (1) Rayleigh, (2) first wind-induced, (3) second wind-induced, and (4) atomization. For laminar turbulent-free cryogenic liquid flow, parameters should be selected to operate within the Rayleigh regime[19] (i.e., $\mathrm{Oh} \ll 1$). In this regime, the fluid column will remain continuous with a smooth surface until the so-called intact length, estimated as follows[20]:

$$l \approx 12v\left(\sqrt{\frac{\rho d_0^3}{\sigma}} + \frac{3\eta d_0}{\sigma}\right)$$

The different fluid parameters for a 5 µm diameter cylindrical cryogenic hydrogen jet operated at 60 psig and 17 K are summarized in **Figure 3**. To maintain a continuous jet for longer distances, the liquid must be cooled sufficiently close to the liquid-solid phase transition (**Figure 4**) so that evaporative cooling, occurring once the jet propagates in vacuum, solidifies the jet before the onset of Rayleigh breakup[3,21].

Protocol

The following protocol details the assembly and operation of a 5 µm diameter cylindrical cryogenic hydrogen jet operated at 17 K, 60 psig as an example case. An extension of this platform to other aperture types and gases requires operation at different pressures and temperatures. As a reference, working parameters for other jets are listed in Table 1. Sections 1-3 and section 7 are performed at ambient temperature and pressure, while sections 4-6 are performed at high vacuum.

1. Installation of the cryostat in the vacuum chamber

CAUTION: A vacuum vessel can be hazardous to personnel and equipment from collapse, rupture due to back-fill pressurization, or implosion due to vacuum window failure. Pressure relief valves and burst disks must be installed on vacuum vessels within a cryogenic system to prevent over-pressurization.

1. Carefully insert the cryostat into the vacuum chamber. Vibrationally isolate the cryostat from the vacuum chamber using a stabilization platform.

2. Perform a vacuum test to determine the baseline vacuum pressure which, we have found, must be better than ~5 x 10^{-5} mBar. A residual gas analyzer (RGA) is often helpful to identify moisture and contaminant gases present in the system.
3. Connect the temperature controller and heater to the cryostat and confirm an accurate reading at ambient temperature.
    1. If an unexpected value is measured, verify continuity from the temperature sensor to the correct terminals on the temperature controller. Otherwise, replace the temperature sensor.
4. Connect the helium return line(s) to an adjustable flow meter panel.
5. Evacuate the insulating vacuum shroud on the transfer line to better than 1 x 10^{-2} mBar using a turbomolecular pump backed by a dry scroll pump.
6. Apply a thin layer of cryogenic vacuum grease to the O-ring inside the head of the cryostat.
7. Slowly insert the transfer line refrigerator bayonet into the cryostat until the adjustment screw contacts the cryostat head. There should be minimal resistance. Tighten the adjustment screw to set the needle valve on the refrigerator bayonet to the desired position.
8. Conduct a cryostat performance test to verify the temperature sensor reliability by cooling down to the lowest attainable temperature. If unexpected temperatures are measured during the cool-down, visually inspect the temperature sensors for good contact with the cryostat. If necessary, reposition and apply cryogenic vacuum grease to improve contact.
9. Assemble the sample gas line according to the P&ID diagram in **Figure 1**. Use a high sensitivity leak detector to identify any leaks.
   CAUTION: Hydrogen, deuterium, and methane are extremely flammable gases. Use piping and equipment designed to withstand the pressures and physical hazards. Local exhaust or ventilation are required to keep the concentration below the explosion limit. Before applying this procedure with any other gases, consult the associated safety data sheet (SDS).
10. Purge the gas line according to the continuous flow purging technique to dilute contaminant gases and water vapor to the purity of the sample gas. The total time depends on the volume of the gas line and gas flow at a given backing pressure.
    CAUTION: While purging the line, ensure the vacuum chamber is adequately ventilated or maintained under vacuum to prevent accumulation of flammable gases.
11. After the initial purge is complete, maintain constant positive pressure (e.g., 30 sccm at 50 psig) on the line to mitigate the risk of contaminant gases entering the line when the vacuum chamber is at ambient pressure.

2. Installation of the cryogenic source components

NOTE: All preparation and assembly of the cryogenic source components should be performed in a clean environment with the appropriate cleanroom clothing (i.e., gloves, hairnets, lab coats, etc.).

1. Use indirect ultrasonic cleaning to remove contaminants (e.g., residual indium) from the cryogenic source components.
    1. Fill a sonicator with distilled water and add a surfactant to reduce the surface tension of the water.
    2. Place cryogenic source parts in individual glass beakers, fully submerge them in electronics-grade isopropanol, and loosely cover the beakers with aluminum foil to reduce evaporation and to prevent particle contamination.
    3. Place the beakers in the cleaning basket or a beaker stand in the sonicator to maximize cavitation. Beakers should not touch the bottom of the sonicator.
    4. Activate the sonicator for 60 min.
    5. Inspect the isopropanol using a bright white light for suspended particles or residue.
    6. If particles are visible, rinse the parts with clean isopropanol, and replace the isopropanol bath. Sonicate in cycles of 60 min until no particles or residue are visible.
    7. Place the parts on a covered, clean surface to desiccate for a minimum of 30 min before assembly.
2. Repeat section 2.1 for the stainless-steel filter, source cap, ferrule, and assembly screws.
3. Cut a piece of indium to maximally cover the junction between the cryogenic source body and cold finger of the cryostat.
4. Place the indium on the cryogenic source and hold it flush with the cold finger of the cryostat. Tighten the retaining screws, ensuring the indium remains flat, to establish a thermal seal between the components. Do not overtighten, as the copper threads are easily damaged.
5. Screw the threaded stainless-steel filter onto the cryogenic source flange.
6. Place an indium gasket on the source flange. Attach the source flange to the cryogenic source body using the flange screws. Tighten the screws diagonally instead of sequentially around the circumference.
7. Connect the sample gas line on the cryostat to the cryogenic source. Check for leaks using a high sensitivity leak detector.

3. Installation of aperture

1. Select an aperture according to experimental needs.
    1. Inspect the aperture using brightfield and darkfield microscopy techniques to identify imperfections in the aperture, physical obstructions, or residual photoresist.
    2. Some physical obstructions can be removed easily when rinsed with isopropanol. Otherwise, discard the aperture.
    3. If there is residual photoresist from the nanofabrication of the aperture, use an acetone bath or piranha solution to remove it.
       CAUTION: Piranha solution, consisting of 3:1 sulfuric acid (H_2SO_4) and hydrogen peroxide (H_2O_2), is extremely corrosive to organic material, including the skin and respiratory tract. The reaction of Piranha with organic material releases gas, which may become explosive. Never seal containers containing Piranha. A full-face shield, chemical resistant apron, lab coat, and neoprene gloves are required.
2. Rinse the aperture with electronics-grade isopropanol to remove any debris or surface contamination. Allow the aperture to dry on a clean and covered surface for 10 min before installation.
3. Place the ferrule inside the cap.
4. Use clean, soft-tipped tweezers to place the aperture inside the ferrule. Tap the cap to center the aperture in the ferrule.
5. Drop an indium ring on top of the aperture. Again, tap the edge of the cap to center the indium ring on the aperture.

6. Hand-tighten the cap onto the source flange until minimal resistance is detected.
7. Derestrict the flow rate on the mass flow controller by increasing the setpoint to 500 sccm and set the gas pressure to ~50 psig on the pressure regulator.
8. Tighten the aperture delicately by a few degrees at a time using a wrench until the flow rate begins to decrease.
9. Finish tightening the cap by checking the leak rate at the top of the cap with the high-sensitivity leak detector instead of the mass flow controller. Stop when tightening no longer decreases the measured leak rate.
10. If the flow rate does not drop below approximately 50 sccm, proceed with the following steps.
    1. Use the leak detector to check for leaks around the source flange and cap. Retighten the screws on the source flange and remeasure the leak rate.
    2. Remove the cap and inspect the aperture and tip of the source flange.
    3. If the aperture is damaged, clean the cap according to step 2.2 and repeat section 3.
    4. If the indium ring is fixed to the aperture, discard the aperture and repeat section 3.
    5. If the complete indium ring is fixed to the flange, use a clean plastic razor blade to scrape off residual indium, then repeat steps 3.2-3.10.
    6. Over time, indium may accumulate on the tip of the source flange preventing subsequent apertures from sealing. In this case, remove the source flange and repeat sections 2.1-2.2 followed by steps 2.5-2.7.
11. As a safety precaution, change the setpoint on the mass flow controller to 10 sccm higher than the final flow determined by the dimensions of the aperture.

4. Cool-down procedure

1. Verify vacuum chamber pressure has reached the expected baseline for a given sample gas flow. To ensure the absence of contaminant gases, which will deposit on the cryogenic source during cool-down, the vacuum chamber is typically pumped for at least 1 h after reaching baseline pressure. This duration varies with local humidity levels and the vacuum system.
2. Turn on the cryostat exhaust heater to prevent frosting of the cryostat head from the return flow of helium gas.
3. Derestrict the gas flow on the mass flow controller by increasing the setpoint to 500 sccm.
4. Fill the open-cycle cold trap with liquid nitrogen. Ensure that the level of liquid nitrogen is above the in-line filter at all times. Monitor and refill as required during cool-down and jet operation.
   CAUTION: Contact with cryogenic liquids, such as liquid nitrogen or liquid helium, will burn the skin, face, and eyes. When handling large volumes of cryogenic liquids (multi-liter), wear a face shield, safety glasses, thermally insulated cryogenic gloves, cryogenic apron, long pants without cuffs, and close-toed shoes. Such liquids may displace oxygen and cause rapid suffocation.
5. Set the adjustable flow meter(s) on the helium return line(s) to fully open.
6. Depressurize the liquid helium dewar using the vent valve.
7. Close the ball valve to the low pressure relief valve on the liquid helium dewar. The recommended dewar pressure during cool-down is 10 psig. An angle valve on the dewar adapter allows the operator to reduce the dewar pressure if there is surplus cooling power after sample liquefaction.
8. Insert the supply dewar bayonet into the liquid helium dewar in one smooth motion. The dewar should pressurize to 10 psig when the bayonet contacts the liquid.
   CAUTION: Keep all exposed skin away from the neck of the dewar at all times.
9. Check for helium gas leaks between the dewar and dewar adapter once the connection has been tightened using a leak detector.
10. Activate the heater on the temperature controller and set the temperature setpoint to 295 K.
11. Once the transfer line fills and cools, the cryostat temperature will drop from ambient temperature to 295 K, at which point the heater will activate to prevent a further drop in temperature. Note that the time required for the initial drop in temperature depends on the dewar pressure and total transfer line and cryostat length.
12. Set the ramp rate on the temperature controller to 0.1 K/s and the setpoint to 200 K. Regulate the helium flow to follow the ramp so the heater does not turn on. Hold at 200 K for a brief dwell segment (e.g., 5 min) to allow the cryostat to thermalize. Repeat for two additional ramp-dwell segments to 120 K then 40 K. A conservative cool-down procedure is used to avoid strong temperature gradients along the system and allows the system parameters to be closely monitored. The dwell temperatures are selected away from sublimation temperatures for contaminant gases.
    1. If the gas flow increases unexpectedly, the indium seal on the source flange or aperture may have failed. Abort the cool-down procedure by proceeding to step 6.4. Once the vacuum chamber has been vented, inspect the seals and refer to section 3.10 to retighten and check for leaks.
13. At 40 K, manually tune the temperature controller P-I-D parameters following the Ziegler-Nichols method[22] until the temperature stability is better than ±0.02 K.

5. Liquefication and jet operation

1. Confirm that the liquid nitrogen level is above the in-line filter.
2. Disable the temperature ramp and change the setpoint temperature to well below the theoretical vapor-liquid phase transition temperature (e.g., 20 K for hydrogen).
3. At the onset of liquefaction, the gas flow will increase up to the maximum and a mixture of gas and liquid will spray from the aperture. Increase the helium flow(s) to provide additional cooling power to quickly pass through the phase transition.
4. Use high magnification shadowgraphy with pulsed, sub-nanosecond illumination to visualize the jet stability and laminarity[23].
5. Optional: If an application or experiment has a pre-determined location for the sample (e.g., detectors aligned to the same position in space), translate the cryogenic source using a multi-axis manipulator on the cryostat flange or motorized push-pin actuators in the vacuum chamber.
6. Translate the catcher to maximize the pressure in the catcher foreline.

7. Optimize the P-I-D parameters and helium flow to improve the temperature stability to better than ±0.02 K. Note that the overall stability of the jet strongly depends on the vacuum chamber pressure, gas backing pressure, and temperature. For example, a change in as little as 1 x 10^{-5} mBar may require reoptimization.
8. Scan in temperature and pressure to optimize the jet stability and laminarity. Sample jet parameters are listed in Table 1.
    1. If the jet breaks up into a spray, the pressure and temperature in phase space may be too close to the vaporization curve.
    2. Large amplitude temperature or helium flow oscillations will result in periodic spatial perturbations, which (in the extreme case) result in driven breakup of the jet. Reduce the helium flow and reoptimize P-I-D parameters to damp the oscillations.
    3. If the jet exhibits transverse (i.e., first-wind regime) or longitudinal waves (i.e., Plateau-Rayleigh instability), decrease the temperature to increase the viscosity, thereby reducing the Reynolds number.
    4. If laminarity cannot be achieved and the jet characteristics are independent of changes in temperature and pressure, there may be a physical obstruction (e.g., physical debris or ice) in the aperture. Before aborting the test, follow steps 6.1-6.5 and closely monitor the vacuum pressure and cryostat temperature. If a contaminant gas or water has sublimated on the aperture causing a partial or full blockage, it can be identified by the boil-off temperature. Repeat steps 4.11-4.12 and 5.1-5.6 to determine if the jet stability improves.

6. Warm-up procedure

NOTE: If the aperture is damaged during operation, immediately limit the sample gas flow to 10 sccm and reduce the sample gas pressure to 30 psig. Then, proceed directly to step 6.5.

1. Change the setpoint to 20 K and decrease the gas pressure from operating pressure to approximately 30 psig.
2. Increase the temperature setpoint in steps of 1 K while monitoring the pressure on the gas regulator. As the liquid in the cryogenic source vaporizes, the pressure in the gas line will rapidly increase and the flow across the mass flow controller will read 0 sccm.
   NOTE: Do not allow the gas pressure to exceed the maximum operating pressure of the components on the sample gas line. If this occurs, wait until the line depressurizes to a safe value through the aperture or pressure relief valve before increasing the setpoint further.
3. Repeat step 6.2 until increasing the temperature setpoint by 1 K does not result in an increase in gas line pressure.
4. Enable the temperature ramp, change the temperature setpoint to 300 K, and regulate the helium flow as required to maintain a temperature increase of 0.1 K/s.
5. Once the source temperature is above 100 K, close the adjustable flowmeter(s) on the helium return line(s). Depressurize the dewar and open the ball valve to the lowest pressure relief valve.
6. Wait until the cryostat thermalizes at 300 K before venting the vacuum chamber. This will prevent water vapor from condensing on the cryostat and cryogenic source components.
7. Depressurize the dewar, then remove the supply dewar bayonet.
8. Remove the liquid nitrogen cold trap.
9. Limit the gas flow on the mass flow controller to 30 sccm.
10. Turn off the exhaust gas heater.
11. Deactivate the heater on the temperature controller.
12. If the aperture is damaged or an obstruction is suspected from a change in flow, proceed to section 7. Otherwise, the aperture does not need to be replaced.

7. Replacement of aperture

1. Remove the cap and inspect the aperture and tip of the source flange.
2. If the indium ring sticks to the flange, use a clean plastic razor blade to scrape it off using moderate pressure.
3. If the aperture remains sealed to the source flange when the cap is removed, limit the gas flow to 10 sccm and confirm the gas backing pressure has dropped to 30 psig. Remove the aperture carefully with a plastic razor blade. If removed prematurely, over-pressurization in the line may damage or eject the aperture.
4. Repeat section 3 to install a new aperture.

Representative Results

Following step 5.4, high magnification shadowgraphs are used to assess laminarity, positioning jitter, and long-term stability during jet operation. It is critical to use pulsed, sub-nanosecond illumination to record an instantaneous image of the jet so that the jet motion (~0.1 µm/ns for H_2) does not blur surface irregularities or turbulence. Sample images of 2 x 20 μm^2 H_2, 4 x 12 μm^2 H_2, and 4 x 20 μm^2 D_2 jets are shown in **Figure 5**.

An additional high magnification imaging system is used to precisely position the cryogenic liquid jet in space. For simplicity, the imaging systems are designed to provide front and side views of the jet. It is particularly important to assess the jet stability and determine the orientation of the planar jets. A study of the spatial jitter of a 2 x 20 μm^2 H_2 as a function of distance from the aperture, performed during a single test over several hours, is shown in **Figure 6**. The 1σ positioning jitter for each datapoint in **Figure 6A** was calculated from 49 images recorded at 10 Hz. Here, the jet position was determined relative to a fixed reference position. **Figure 6B** shows the normalized histograms of the jet position at 23 mm as an example. A more detailed study can be found in Obst et al.[5]. On average, the spatial jitter increases linearly away from the nozzle.

Typical system observables during liquefying and jet operation (according to section 5) of a 4 x 20 μm^2 cryogenic deuterium jet are shown in **Figure 7**. Careful monitoring of the temperature, flow, sample backing pressure, and vacuum pressures allows the operator to quickly identify any irregularities and react accordingly. For example, if the jet leaves the catcher, indicated by a dashed box, the vacuum chamber and foreline pressure increase significantly. Additional cooling power is then needed to maintain the setpoint temperature.

Once stabilized, all observables should be constant with minimal oscillations. Any long-term drift is indicative of a problem (e.g., leaks, gas contamination, decrease in vacuum system performance, positioning drift in catcher). The choice of aperture strongly dictates the operational parameters of the jet in the Rayleigh regime. Once the optimal parameters are identified for a given gas and aperture type, the resulting jet is highly reproducible; however, any minor deviations in the aperture require reoptimization starting from the previously identified values. Typical operation parameters are summarized in **Table 1**.

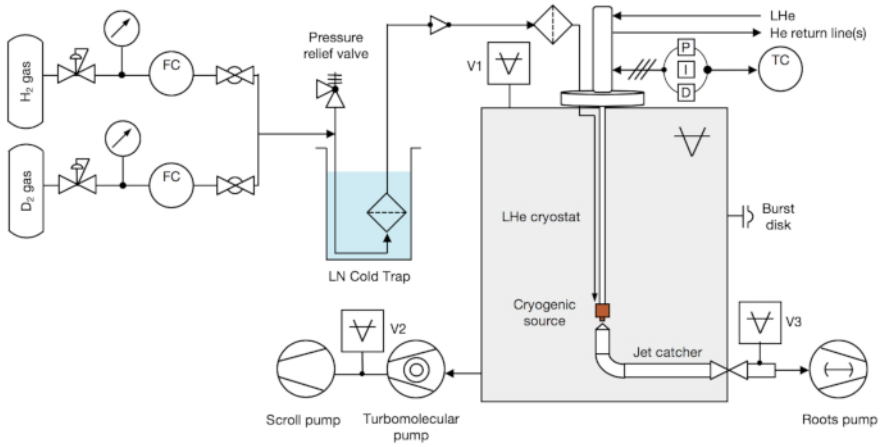

Figure 1: P&ID diagram of a typical cryogenic liquid jet delivery platform. The sample gas, vacuum, and cryogenic subsystems are depicted. The vacuum chamber, turbomolecular pump foreline, and jet catcher foreline pressures are monitored with vacuum gauges V1, V2, and V3, respectively. The cryostat temperature is actively regulated using a P-I-D temperature controller. Please click here to view a larger version of this figure.

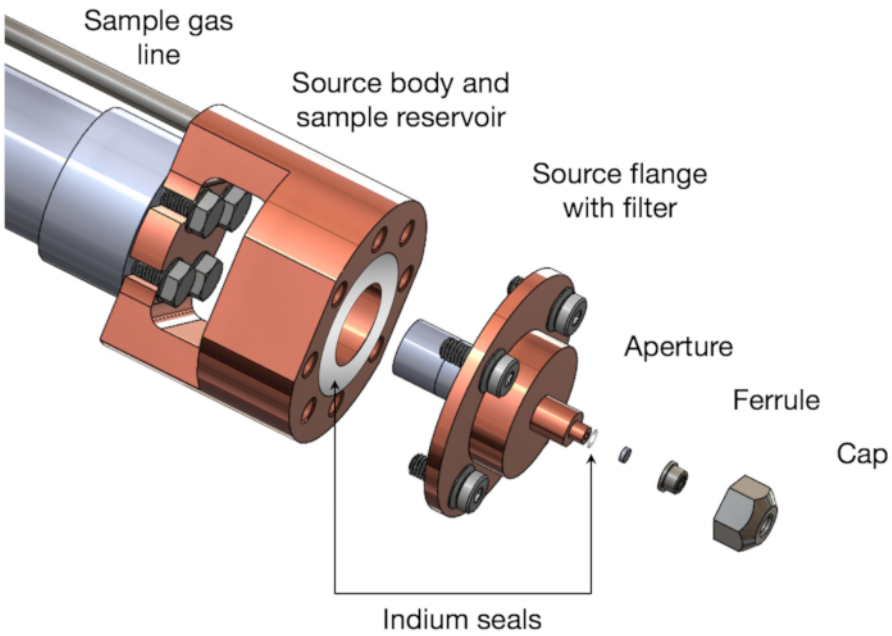

Figure 2: Three-dimensional exploded-view drawing of the cryogenic source assembly. Indium seals are installed between the cold finger and source body, source body and flange, and source flange and aperture. Please click here to view a larger version of this figure.

Density[15]	ρ	74.42 kg/m^3
Velocity	v	121 m/s
Viscosity[15]	η	18.583E-6 Pa s
Surface tension[15]	σ	2.4958E-3 N/m
Reynolds number	R_e	2422
Weber number	W_e	2183
Ohnesorge number	Oh	1.928E-2
Intact length	l	2.43 mm

Figure 3: Summary of fluid dynamics parameters. Parameters are provided, assuming a ø5 µm cylindrical cryogenic hydrogen jet operated at 60 psig and 17 K. Values for density, viscosity, and surface tension are from NIST.[15]. Please click here to view a larger version of this figure.

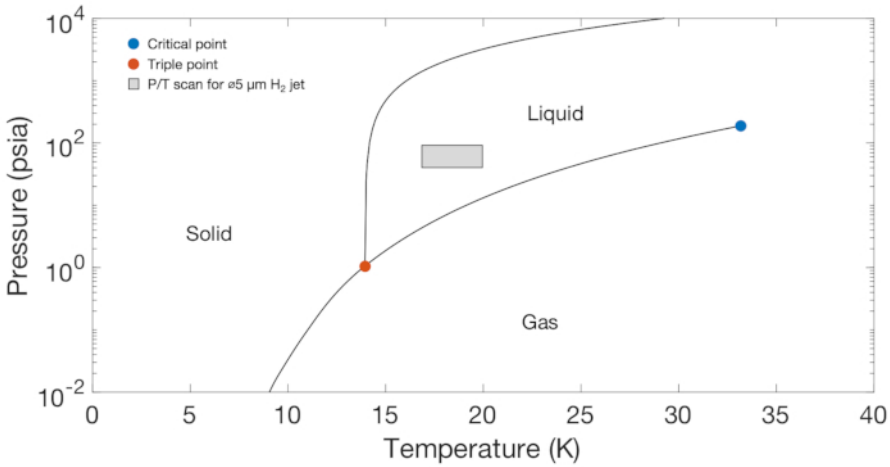

Figure 4: Hydrogen equation of state at cryogenic temperatures[15]. The critical and triple points are indicated by blue and orange filled circles, respectively. Jet operation follows an isobar through the gas-liquid phase transition. The jet solidifies via evaporative cooling in the vacuum chamber. The grey box indicates the range of backing pressures (40-90 psia) and temperatures (17-20 K) which are scanned over to optimize the stability of a ø5 µm cylindrical cryogenic hydrogen jet. Please click here to view a larger version of this figure.

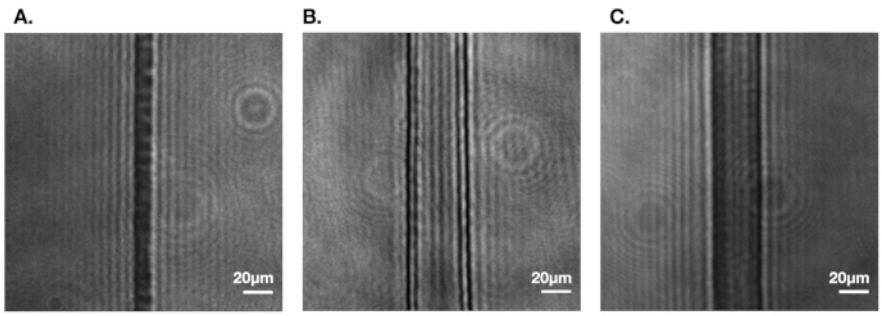

Figure 5: Representative 20x magnification shadowgraphs of turbulent-free, laminar cryogenic liquid jetsusing a 10 ps/1057 nm wavelength laser. (**A**) Aperture = 2 x 20 µm^2, gas = H_2, T = 15.8 K, P = 188 psig. (**B**) Aperture = 4 x 12 µm^2, gas = H_2, T = 17.2 K, P = 80 psig. (**C**) Aperture = 4 x 20 µm^2, gas: D_2, T = 20 K, P = 141 psig. Please click here to view a larger version of this figure.

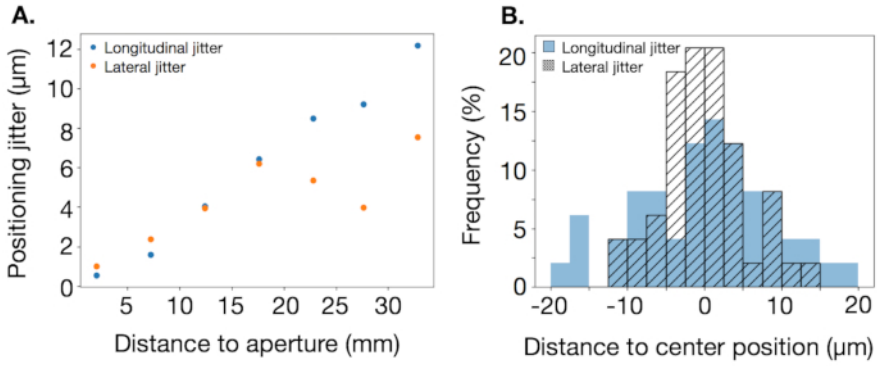

Figure 6: Jet position stability for 2 x 20 μm^2 cryogenic hydrogen jet. Parameters are 18 K, 60 psig, and $R_e \approx 1887$. (**A)** Positioning jitter as a function of distance from the aperture. The longitudinal (lateral) jitter corresponds to motion parallel to the short (long) axis of the rectangular sheet. (**B)** Normalized histogram of jet position to determine the lateral jitter (σ = 5.5 μm) and longitudinal jitter (σ = 8.5 μm) 23 mm from the nozzle. Please click here to view a larger version of this figure.

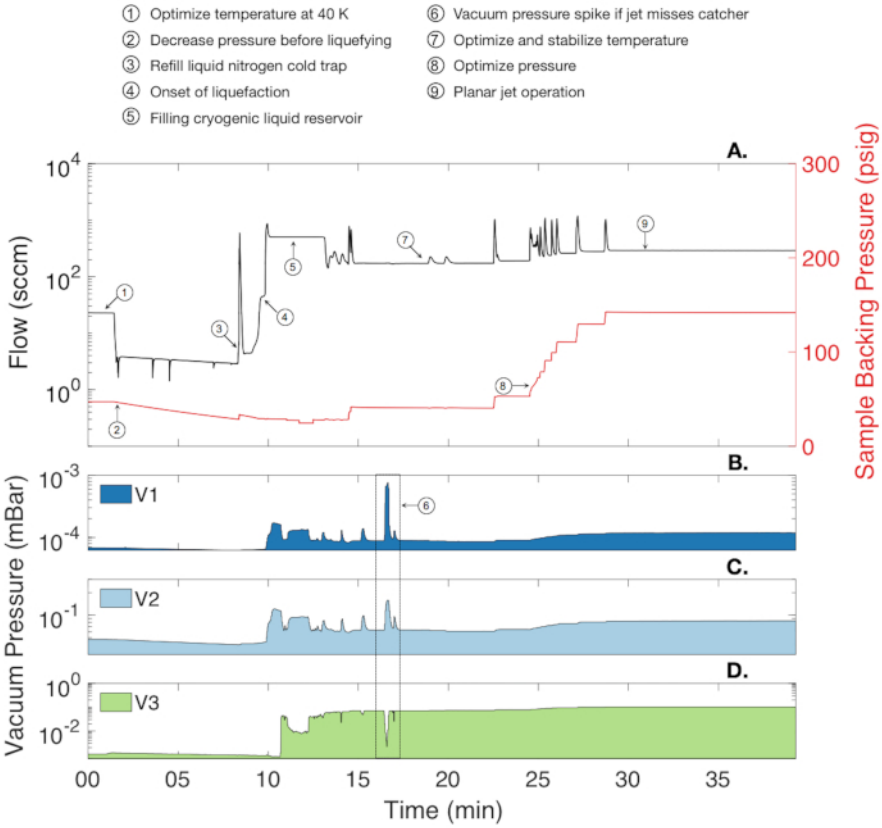

Figure 7: Representative flow and pressures during cryogenic jet operation. (**A**) Left: sample gas flow, right: sample gas backing pressure as a function of time. Semi-log plot of the vacuum chamber pressure (V1; **B**), turbomolecular pump foreline pressure (V2; **C**), and jet catcher pressure (V3; **D**) as functions of time. Circled numbers identify changes in the system observed during section 5 of the protocol. Please click here to view a larger version of this figure.

Sample gas	Aperture	Temperature (K)	Pressure (psig)	Flow (sccm)
Hydrogen	ø5 µm cylindrical	17	60	150
50% Hydrogen, 50% Deuterium	ø5 µm cylindrical	20	30, 30	130
Deuterium	ø5 µm cylindrical	22	75	80
Hydrogen	1 µm x 20 µm planar	18	182	150
Hydrogen	2 µm x 20 µm planar	18	218	236
Hydrogen	4 µm x 20 µm planar	17.5	140	414
Deuterium	4 µm x 20 µm planar	20.5	117	267
Argon	ø5 µm cylindrical	90	50	18.5
Methane	ø5 µm cylindrical	100	75	46

Table 1: Sample jet operation conditions.

Discussion

Successful operation of the cryogenic liquid jet requires meticulous cleanliness and careful monitoring of temperature stability. One of the most frequent and avoidable failures is a partial or full blockage of the micron-sized aperture. Copper, stainless steel, or indium from the source or airborne particles can be introduced at any step of the source assembly. All components must undergo a robust cleaning process using indirect sonication. Assembly and storage in a Class-10,000 cleanroom or better improves the success rate.

Another critical step of the procedure is to stabilize the cryogenic source temperature. Users must ensure that the temperature of the liquid exiting the source is measured independently from the variable heat released by continuous liquefaction in the reservoir. This is accomplished by placing the temperature sensor near the aperture (e.g., on the source flange) or far from the heat source. Furthermore, P-I-D parameters must be manually optimized using the Ziegler-Nichols method for each combination of temperature and backing pressure. If the temperature fluctuations become too large, periodic oscillations can be observed on the jet sometimes leading to periodic breakup. It should be noted that built-in autotuning functions or low-pass filters have not been successful in stabilizing the temperature during jet operation.

The cryogenic liquid jet system, while highly adaptable, is challenging to implement at large-scale facilities with established vacuum protocols. For instance, differential pumping stages are required when upstream equipment is sensitive to the residual gas (e.g., FLASH free-electron laser at DESY or MeV-UED instrument at SLAC). In addition, large diameter vacuum chambers, such as those for multi-PW lasers, likely require in-vacuum flexible cryostats. Compared to conventional fixed length cryostats, they can be readily decoupled from chamber vibrations and have a shorter lever arm. A flexible in-vacuum cryostat has already been implemented with the Draco Petawatt laser at Helmholtz-Zentrum Dresden-Rossendorf (HZDR). Another observation is that the aperture can be damaged when the jet is irradiated by an ultra-high intensity laser too close to the source. Recently, a mechanical chopper blade (operating at 150 Hz and synchronized with the laser pulse) has been implemented to protect and isolate the aperture from the laser-plasma interaction.

This system produces micron-scale, highly tunable, turbulent-free, laminar cylindrical and planar cryogenic liquid jets. Ongoing development of the cryogenic liquid jet system is focused on advanced aperture materials and design, vacuum system and catcher improvements, and advanced hydrogen isotope mixing. This system will enable a transition to high repetition rate high energy density science and pave the way to the development of next-generation particle accelerators.

Disclosures

The authors have nothing to disclose.

Acknowledgments

This work was supported by the U.S. Department of Energy SLAC Contract No. DE- AC02-76SF00515 and by the U.S. DOE Office of Science, Fusion Energy Sciences under FWP 100182. This work was also partially supported by the National Science Foundation under Grant No. 1632708 and by EC H2020 LASERLAB-EUROPE/LEPP (Contract No. 654148). C.B.C. acknowledges support from the Natural Sciences and Engineering Research Council of Canada (NSERC). F.T. acknowledges support from National Nuclear Security Administration (NNSA).

References

1. Gauthier, M. et al. High repetition rate, multi-MeV proton source from cryogenic hydrogen jets. *Applied Physics Letters.* **111**, 114102 (2017).
2. Grisenti, R. E. et al. Cryogenic microjet for exploration of superfluidity in highly supercooled molecular hydrogen. *Europhysics Letters.* **73**, 540–546 (2006).
3. Kim, J. B., Göde, S., Glenzer, S. H. Development of a cryogenic hydrogen microjet for high-intensity, high repetition rate experiments. *Review of Scientific Instruments.* **87**, 11E328 (2016).
4. Gauthier, M. et al. High-intensity laser-accelerated ion beam produced from cryogenic micro-jet target. *Review of Scientific Instruments.* **87**, 11D827 (2016).

5. Obst, L. et al. Efficient laser-driven proton acceleration from cylindrical and planar cryogenic hydrogen jets. *Scientific Reports.* **7**, 10248 (2017).
6. Goede, S. et al. Relativistic Electron Streaming Instabilities Modulate Proton Beams Accelerated in Laser-Plasma Interactions. *Physical Review Letters.* **118**, 194801 (2017).
7. Kühnel, M. et al. Time-Resolved Study of Crystallization in Deeply Cooled Liquid Parahydrogen. *Physical Review Letters.* **106**, 245301 (2011).
8. McBride, E. E. et al. Setup for meV-resolution inelastic X-ray scattering measurements and X-ray diffraction at the Matter in Extreme Conditions endstation at the Linac Coherent Light Source. *Review of Scientific Instruments.* **HTPD2018**, 10F104 (2018).
9. Glenzer, S. H. et al. Matter under extreme conditions experiments at the Linac Coherent Light Source. *Journal of Physics B: Atomic, Molecular and Optical Physics.* **49**, 9 (2016).
10. Garcia S., Chatain D., Perin, J. P. Continuous production of a thin ribbon of solid hydrogen. *Laser and Particle Beams.* **32**, 569-575 (2014).
11. Margarone, D. et al. Proton Acceleration Driven by a Nanosecond Laser from a Cryogenic Thin Solid-Hydrogen Ribbon. *Physical Review X*. **6**, 041030 (2016).
12. Kraft, S. et al. First demonstration of multi-MeV proton acceleration from a cryogenic hydrogen ribbon target. *Plasma Physics and Controlled Fusion.* **60**, 044010, (2018).
13. Polz, J. et al. Efficient Laser-Driven Proton Acceleration from a Cryogenic Solid Hydrogen Target. *Scientific Reports.* **9**, 16534 (2019).
14. Kim, J. B., Schoenwaelder, C., Glenzer, S. H. Development and characterization of liquid argon and methane microjets for high-rep-rate laser-plasma experiments. *Review of Scientific Instruments.* **89**, 10K105 (2018).
15. *NIST Standard Reference Database Number 69*. https://doi.org/10.18434/T4D303. (2018).
16. Corruccini, R. J. Gaseous heat conduction at low pressures and temperatures. *Vacuum.* **7-8**, 19-29 (1959).
17. Scott, R. B., Denton W. H., Nicholls, C. M. *Technology and Uses of Liquid Hydrogen.* Pergamon Press Ltd. (1964).
18. Ha, B., DePonte, D., Santiago, G. Device design and flow scaling for liquid sheet jets. *Physical Review Fluids*. **3**, 114202 (2018).
19. Eggers, J., Villermaux, E. Physics of liquid jets. *Rep. Prog. Phys.* **71,** 036601 (2008).
20. McCarthy, M. J., Molloy, N. A. Review of Stability of Liquid Jets and the Influence of Nozzle Design. *Chemical Engineering Journal.* **7**, 1-20 (1974).
21. Neumayer, P. et al. Evidence for ultra-fast heating in intense laser irradiated reduced-mass targets. *Physics of Plasmas.* **19**, 122708 (2012).
22. Ziegler, J. G., Nichols, N. B. Optimum Settings for Automatic Controllers. *Transactions of the American Society of Mechanical Engineers*. **64**, 759–768 (1942).
23. Ziegler, T. et al. Optical probing of high intensity laser interaction with micron-sized cryogenic hydrogen jets. *Plasma Physics and Controlled Fusion.* **60**, 074003 (2018).